the associated backflow necessary to establish current continuity. Our results suggest the existence of an effect such that the actual driving force on a flux line is given by $J\varphi_0/c$ multiplied by a function depending only on the ratio of the current in the core to the transport current.

The possibility that η varies with current has been ignored in our discussion. From the form of (4) we could not distinguish this from the variation of g. However, it follows from Bardeen's work[4] that a dependence of η on current will occur only when the normal current in the core is no longer negligible compared with the vortex supercurrent. In the low-current nonlinear region we would expect η to be strictly current independent.

*Work supported by the U. S. Air Force of Scientific Research through Grant No. AFOSR 565-64.

[1]Y. B. Kim, C. F. Hempstead, and A. R. Strnad, Phys. Rev. 139, A1163 (1965).

[2]M. J. Stephen and J. Bardeen, Phys. Rev. Letters 14, 112 (1965).

[3]J. Friedel, P. G. de Gennes, and J. Matricon, Phys. Letters 2, 119 (1963).

[4]J. Bardeen, Phys. Rev. Letters 13, 747 (1964).

FERMI SURFACE, MAGNETIC ORDERING, AND ELECTRICAL PROPERTIES OF RARE-EARTH METALS

A. J. Freeman

National Magnet Laboratory,* Massachusetts Institute of Technology, Cambridge, Massachusetts

and

J. O. Dimmock

Lincoln Laboratory,† Massachusetts Institute of Technology, Lexington, Massachusetts

and

R. E. Watson

Brookhaven National Laboratory,‡ Upton, New York

(Received 15 December 1965)

This Letter presents the complete Fermi surface for Tm metal determined from nonrelativistic augmented plane-wave (APW) energy-band calculations. The computed energy bands are of mixed s-d character and strongly resemble those of the transition metals in this aspect. The computed Fermi surface is determined largely by the d bands and bears no resemblance to that of the free-electron model. The striking anomalies which occur in the c-axis resistivity of the heavy rare-earth metals at the onset of long-range periodic magnetic order are found to be understandable using our energy-band and Fermi-surface results. We find that the observed $\vec{q}$ vector spans a section of the calculated Fermi surface of Tm such that a section of this Fermi surface perpendicular to the z axis is destroyed at the onset of magnetic ordering. This results in the observed resistivity anomaly at T_N. Also, due to the fact that the energy bands are relatively flat in the vicinity of the Fermi energy, we indicate that sizable gaps occur at superzone boundaries for $k_z = \pm\frac{1}{2}nq$ as the temperature is lowered below T_N, thereby destroying large sections of the Fermi surface normal to the z axis.

Information about the Fermi surface of rare-earth metals is indispensable for understanding many of the electronic and some of the magnetic properties of this important class of materials. One such property of recent interest is the electrical resistivity which shows anomalies in its temperature dependence.[1] These anomalies have been successfully interpreted by Mackintosh,[2] Elliott and Wedgewood,[3] Miwa,[4] and others in terms of the magnetic ordering of these materials. In this view, the anomaly in the electrical resistivity along the c axis, which occurs at the antiferromagnetic ordering temperature, is associated with band gaps introduced by superzone boundaries arising from the onset of the long-range periodic magnetic order. Good agreement has been obtained

between theory and experiment using the free-electron model of the conduction bands and the associated Fermi surface. This agreement has since been taken as evidence in support of the validity of the free-electron model. However, the recent determination,[5] by means of APW calculations, that the conduction bands in Gd resemble those of the transition metals and differ markedly from free-electron bands showed that this model was completely invalid for the rare-earth metals. It also raised the question at the same time as to whether agreement between theory and experiment could be restored using the APW band structure and the resulting Fermi surface.

Tm shows a linear spin-wave type structure between 50 and 40°K in which the magnitude of the z component of the moments varies sinusoidally with distance along the c axis. The period of the wave vector is constant at seven (hexagonal) layers over the observed temperature range and differs from that of many of the other rare-earth structures which have periods incommensurate with the lattice and which vary with temperature. This periodic magnetic structure introduces planes of energy discontinuity (superzone gaps) into the nonmagnetic Brillouin-zone structure.[2-4] These energy gaps may affect drastically the electrical conduction of the metal as the temperature is lowered through the Néel temperature provided one of these superzone boundaries destroys a large part of the Fermi surface. The observation of large anisotropy in the resistivity (maximum along the c axis) and the reduction of the anomaly in Tb when the sample is cooled in a magnetic field (which suppresses the long-range order and reduces the band gaps) provided confirmation for the validity of the model.[2] The existence of superzone planes which cut large sections of the Fermi surface in the free-electron model led easily to an explanation of the resistivity anomaly along the c axis and to the variation in resistivity with the variation in magnetic period. The usual argument, based on first-order perturbation theory, asserts that energy gaps and superzone boundaries occur at values of $\vec{k}$ for which

$$E(\vec{k})-E(\vec{k}\pm\vec{q})=0, \tag{1}$$

when the system is subjected to a perturbation of the wave vector $\vec{q}$. Experimentally, $\vec{q}$ lies parallel to the crystal c axis in the rare-earth metals. Since by symmetry $E(\vec{k})=E(-\vec{k})$, this results in planar superzone boundaries at $k_z=\pm\frac{1}{2}q$ or, more completely, at $k_z=\frac{1}{2}K_z\pm\frac{1}{2}q$, where K_z is the z component of a reciprocal lattice vector. It should be noted that although these are the only superzone boundaries required by symmetry, to this order, in general, other boundaries may occur at values of $\vec{k}$ which satisfy Eq. (1) and that these values of $\vec{k}$ will depend specifically on the energy-band structure or, alternatively, on the particular Fermi surface. Specifically, gaps occur at those values of $\vec{k}$ where both $\vec{k}$ and $\vec{k}\pm\vec{q}$ lie on the Fermi surface, that is where $\vec{q}$ spans a section of the Fermi surface.

All of this discussion is limited to first-order perturbation theory, which should be applicable in the vicinity of the ordering temperature where the magnetic moment is small. However, at lower temperatures, if the periodic perturbation is large, compared to the separations between energy bands, a higher order treatment must be considered. In Tm at low temperature, the energy gaps introduced at the superzone boundaries should be about 0.17 eV wide.[6] This energy is comparable to the separation between the flat d bands in the vicinity of the Fermi surface which we have obtained for the rare-earth metals. So-called higher order terms in perturbation theory will introduce energy gaps of magnitude comparable to those at $k_z=\pm\frac{1}{2}q$. Therefore, because of the fact that these bands are relatively flat and closely spaced, we must replace Eq. (1) by

$$E(\vec{k})-E(\vec{k}\pm n\vec{q})=0. \tag{2}$$

This, then, leads to superzone boundaries at $k_z=\pm\frac{1}{2}nq$.

Shown in Fig. 1 is the complete hole surface for Tm metal determined from our APW calculations. We use the double zone representation which is valid for the hcp structure in the absence of spin-orbit coupling. This surface is completely different from the free-electron Fermi surface,[7] which consists of two disconnected hole volumes. Figure 2 shows several vertical cross sections of the Fermi surface. The horizontal lines denote superzone boundaries at $k_z=\pm n(2\pi/7c)$ introduced by the periodic magnetic ordering. The expected distortion of the Fermi surface at $T=0$ is given approximately by the heavy solid curves. The largest portions of the Fermi surface are de-

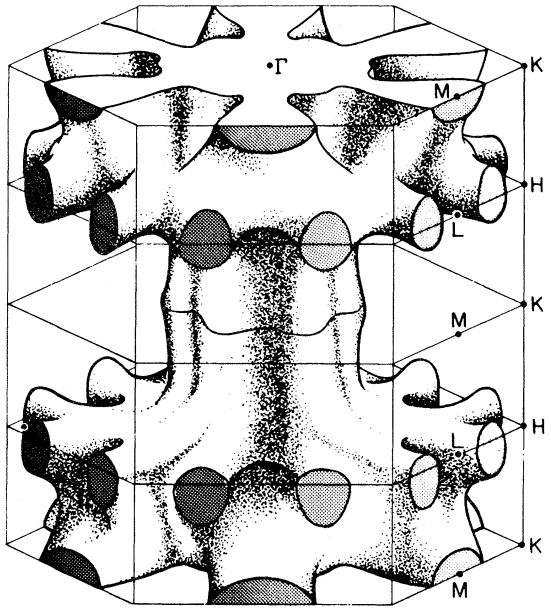

FIG. 1. The complete Fermi surface for holes in Tm metal in the double zone representation.

stroyed by the superzone boundary corresponding to $n = 3$. Notice that this effect is a direct consequence of the presence of several relatively flat d bands in the vicinity of the Fermi energy and would not occur to any extent in the free-electron model. Notice further that the vector $\vec{q} = 4\pi/7c$ actually spans a section of the calculated Fermi surface as can be seen in Fig. 2(b). This is essential to the resistivity anomaly at the transition temperature as discussed above.

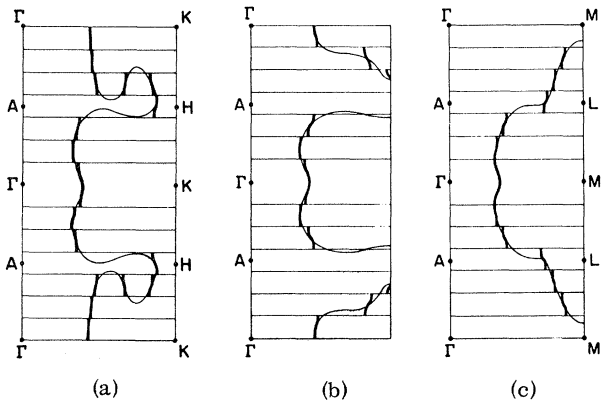

FIG. 2. Some vertical cross sections of the Tm Fermi surface containing the c axis. The influence of magnetic ordering is demonstrated by comparing the low-temperature cross sections, shown as heavy solid curves, with the high-temperature cross sections, shown as light solid curves. The horizontal lines denote superzone boundaries at $k_z = \pm n(2\pi/7c)$ introduced by the magnetic ordering.

In Fig. 2, we have drawn the perturbed Fermi surface in such a way as to emphasize its relationship to the unperturbed surface (the light solid curves). It should be recognized that the Bloch states which originally had unique k values within the double Brillouin zone for the hcp structure are now mixtures of k values differing by multiples of q. Therefore, the assignment of a particular one-electron state to a particular point in k space is ambiguous to this degree. However, the essential feature of the result is that, in the magnetic state, the Fermi surface normal to the z axis is largely destroyed while segments parallel to the axis remain, though somewhat perturbed. This implies a resistance anomaly parallel but not perpendicular to the crystal c axis, in agreement with experiment. It should be pointed out, however, that the calculations we have performed are all nonrelativistic and that relativistic corrections, including spin-orbit effects, will certainly modify, to some extent, the computed Fermi surface. Nevertheless, we feel that the general features of the Fermi surface, as shown in Fig. 1, and of the effects of magnetic ordering, as shown in Fig. 2, should remain even when the relativistic effects are taken into account. It thus appears that the anomalies in the temperature dependence of the resistivity of the heavy rare-earth metals can be understood in terms of the calculated energy bands of these materials, and that qualitative agreement, at least, exists between theory and experiment.

We are indebted to Mrs. A. Furdyna who participated fully in many parts of this work. We are grateful to J. H. Wood for making the APW programs available to us and for many helpful discussions, and to A. Furdyna and R. Sheshinski for their help with many phases of the computations.

*Work supported by the U. S. Air Force Office of Scientific Research.

†Operated with support from the U. S. Air Force.

‡Work supported by the U. S. Atomic Energy Commission.

[1]P. M. Hall, S. Legvold, and F. H. Spedding, Phys. Rev. 109, 971 (1958); R. V. Colvin, S. Legvold, and F. H. Spedding, Phys. Rev. 120, 741 (1960); D. E. Hegland, S. Legvold, and F. H. Spedding, Phys. Rev. 131. 158 (1963).

[2]A. R. Mackintosh, Phys. Rev. Letters 9, 90 (1962).
[3]R. J. Elliott and F. A. Wedgwood, Proc. Phys. Soc. (London) 81, 846 (1963).
[4]H. Miwa, Progr. Theoret. Phys. (Kyoto) 29, 477 (1963).
[5]J. O. Dimmock and A. J. Freeman, Phys. Rev. Letters 13, 750 (1964).
[6]J. O. Dimmock, A. J. Freeman, and R. E. Watson, in Proceedings of the Conference on the Optical Properties and Band Structure of Metals and Alloys, Paris, 1965 (to be published).
[7]W. A. Harrison, Phys. Rev. 118, 1190 (1960).

PHONON SCATTERING BY LATTICE VACANCIES*

J. W. Schwartz and C. T. Walker

Physics Department, Northwestern University, Evanston, Illinois
(Received 1 December 1965)

The existence of impurity resonant-scattering states lying in the acoustic band is comparatively well established. Such states have been observed in thermal conductivity measurements,[1] far-infrared measurements,[2] and recently by inelastic neutron scattering.[3] One particularly interesting impurity which is expected to produce an in-band state is the lattice vacancy. Theoretical calculations[4] suggest that the peak in the phonon-scattering cross section for vacancies should be very sharp, and should be well down in the acoustic band. A phonon-vacancy resonant interaction has not been seen experimentally as it has proved to be quite difficult to produce vacancies in large enough quantities to give a detectable effect.

We wish to report low-temperature thermal-conductivity measurements which we believe demonstrate a resonant scattering of phonons by lattice vacancies. Further, the peak in the scattering cross section seems to occur at the phonon frequencies predicted theoretically, and the measured thermal conductivity curves agree rather well with the predicted ones.

The systems studied were KCl doped with $CaCl_2$, $SrCl_2$, $EuCl_2$, or $BaCl_2$. In these cases the lattice vacancy is a positive-ion vacancy which accompanies the divalent impurity ion. It is known that after proper heat treatment, the vacancy is located in a positive-ion position nearest to the divalent ion. One would anticipate that any resonant-scattering states produced by this system would be complicated indeed since the scattering center contains both a vacancy and a foreign ion. However, the experimental data suggest a far simpler interpretation, namely that the dominant member of the combination is the vacancy, and the divalent ion is seen only as a perturbation on the vacancy effects.

The data are presented in Fig. 1, which shows

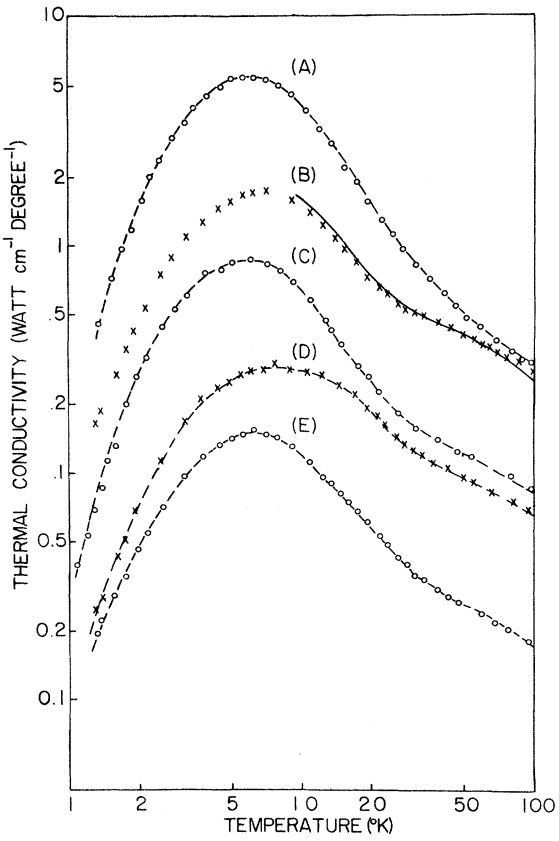

FIG. 1. Thermal conductivity versus temperature for pure and doped KCl. Curve *A*, pure KCl; Curve *B*, KCl:$BaCl_2$; Curve *C*, KCl:$EuCl_2$; Curve *D*, KCl:$SrCl_2$; Curve *E*, KCl:$CaCl_2$. All dopings are in the range 200-300 ppm. Solid line through *B* is a theoretical curve calculated from Krumhansl's cross section using Callaway's model (see Refs. 4 and 5). Dashed lines are experimental curves. *A* and *B* are actual data; for convenience, the original data have been multiplied by 0.29 to give Curve *C*, by 0.29 to give Curve *D*, and by 0.07 to give Curve *E*.